A Section 508–conformant HTML version of this article is available at https://doi.org/10.1289/EHP1318.

Adipogenic Effects and Gene Expression Profiling of Firemaster® 550 Components in Human Primary Preadipocytes

Emily W.Y. Tung, Vian Peshdary, Remi Gagné, Andrea Rowan-Carroll, Carole L. Yauk, Adéle Boudreau, and Ella Atlas

Environmental Health Science and Research Bureau, Health Canada, Ottawa, Ontario, Canada

Background: Exposure to flame retardants has been associated with negative health outcomes including metabolic effects. As polybrominated diphenyl ether flame retardants were pulled from commerce, human exposure to new flame retardants such as Firemaster® 550 (FM550) has increased. Although previous studies in murine systems have shown that FM550 and its main components increase adipogenesis, the effects of FM550 in human models have not been elucidated.

Objectives: The objectives of this study were to determine if FM550 and its components are active in human preadipocytes, and to further investigate their mode of action.

Methods: Human primary preadipocytes were differentiated in the presence of FM550 and its components. Differentiation was assessed by lipid accumulation and expression of peroxisome proliferator-activated receptor γ (PPARG), fatty acid binding protein (FABP) 4 and lipoprotein lipase (LPL). mRNA was collected for Poly (A) RNA sequencing and was used to identify differentially expressed genes (DEGs). Functional analysis of DEGs was undertaken in Ingenuity Pathway Analysis.

Results: FM550 triphenyl phosphate (TPP) and isopropylated triphenyl phosphates (IPTP), increased adipogenesis in human primary preadipocytes as assessed by lipid accumulation and mRNA expression of regulators of adipogenesis such as PPARγ, CCAAT enhancer binding protein (C/EBP) α and sterol regulatory element binding protein (SREBP) 1 as well as the adipogenic markers FABP4 LPL and perilipin. Poly (A) RNA sequencing analysis revealed potential modes of action including liver X receptor/retinoid X receptor (LXR/RXR) activation, thyroid receptor (TR)/RXR, protein kinase A, and nuclear receptor subfamily 1 group H members activation.

Conclusions: We found that FM550, and two of its components, induced adipogenesis in human primary preadipocytes. Further, using global gene expression analysis we showed that both TPP and IPTP likely exert their effects through PPARG to induce adipogenesis. In addition, IPTP perturbed signaling pathways that were not affected by TPP. https://doi.org/10.1289/EHP1318

Introduction

Stringent flammability standards set in the state of California resulted in the widespread use of chemical flame retardants in commercial products (Dodson et al. 2012). Of these, the polybrominated diphenyl ethers (PBDEs) were among the most abundantly used; however, due their toxicity and bioaccumulative properties, they were phased out of commerce. As such, industry was required to find alternatives such as the proprietary mixture Firemaster® 550 (FM550), which is used in commercial products including furniture, textiles, and electronics (Belcher et al. 2014; Stapleton et al. 2008).

FM550 is composed of four different compounds: *bis*(2-ethylhexyl)-2,3,4,5-tetrabromophthalate (TBPH) (8%), 2-ethylhexyl-2,3,4,5-tetrabromobenzoate (TBB) (30%), triphenyl phosphate (TPP) (17%), and isopropylated triphenyl phosphates (IPTPs) (45%) (Stapleton et al. 2008). The IPTPs consist of a mixture of mono-isopropylphenyl, diphenyl-phosphate, di-isopropylphenyl, phenyl-phosphate, and tris-isopropylphenyl-phosphate in various proportions (Phillips et al. 2016). Measurement of the FM550 metabolites diphenyl-phosphate (DPHP) and isopropyl-diphenyl-phosphate (ip-DPHP) in urine confirmed that exposure to the chemical mixture FM550 is ubiquitous (Hoffman et al. 2014). In addition, recent studies show that some of the FM550 components concentrations can reach 15,030 ng/g in house dust (Stapleton 2008) and that the metabolite ip-DPHP is ubiquitous in the urine of children at concentrations up to 24 ng/mL (Hoffman et al. 2014).

A few studies suggest that FM550 and its components have metabolic effects and act as environmental obesogens. For example, in a rodent model, perinatal and lactational exposure to FM550 induced behavioral and endocrine effects, increased adipose mass, and induced insulin resistance in the offspring (Patisaul et al. 2013). In addition, a study in murine stem cells showed that the FM550 components TPP and IPTP divert osteogenesis to the adipogenesis pathway through activation of peroxisome proliferator-activated receptor γ (PPARγ) (Pillai et al. 2014).

Although aforementioned studies (Patisaul et al. 2013; Pillai et al. 2014) suggest that FM550 is an endocrine disruptor and an environmental obesogen in murine cell cultures and animal models, little is known regarding its effects on human health and obesity. Primary human preadipocytes are a relevant tool to test the ability of chemicals to induce adipogenesis in human specimens and hence can identify a potential role for these chemicals to cause metabolic effects in humans (Boucher et al. 2014a; Boucher et al. 2014b). Previous work showed that the transcriptional cascade differs in human and murine differentiating preadipocytes (Tomlinson et al. 2006, 2010). This suggests that chemicals have potentially different specific targets in human cells compared with mouse cells. Further, human preadipocytes have different requirements for optimal differentiation compared with the mouse models (Tomlinson et al. 2006). One major difference is the requirement of clonal expansion for the murine cell model (3T3-L1) but not for the human primary preadipocytes (Janderová et al. 2003; Yeh et al. 1995). In addition, human primary preadipocytes require both dexamethasone (glucocorticoid agonist) and troglitazone (PPARG agonist) to induce differentiation (Janderová et al. 2003). As such, this model presents us with the opportunity to investigate whether the chemicals of interest are acting through PPARG activation or through the glucocorticoid pathway. Conversely, murine 3T3-L1 preadipocytes

Address correspondence to E. Atlas, Environmental Health Science and Research Bureau, Health Canada, 50 Colombine Driveway, Ottawa, Ontario, K1A 0K9, Canada. Telephone: 613-668-6151. Email: ella.atlas@canada.ca

Supplemental Material is available online (https://doi.org/10.1289/EHP1318).

The authors declare they have no actual or potential competing financial interests.

Received 2 November 2016; Revised 18 May 2017; Accepted 23 May 2017; Published 14 September 2017.

differentiate with either dexamethasone or a PPARG agonist (Ahmed and Atlas 2016). Finally, human preadipocytes are primary cells, and therefore provide an *in vitro* model that is more relevant to the human condition and relevant for obesogen screening.

The purpose of this study was to determine the effects of FM550 and its individual components on adipogenesis in human primary preadipocytes, and to explore modes of action through analysis of global transcriptomic response to these chemicals. We show that FM550 and its two major components, TPP and IPTP, induce adipogenesis in human primary cells. Furthermore, global gene expression analysis revealed that pathways other than PPARG may also be involved in the adipogenic changes induced in differentiating human cells in response to FM550 components.

Materials and Methods

Reagents

Chemicals were purchased from the following manufacturers: human insulin (Roche Diagnostics, Indianapolis, IN, USA); 3-isobutyl-1-methylxanthine (IBMX), dexamethasone (DEX), troglitazone, triphenyl phosphate (TPP), and dimethyl sulfoxide (DMSO) (Sigma-Aldrich, Oakville, Ontario, Canada); 2-ethylhexyl-2,3,4,5-tetrabromobenzoate (TBB) and *bis*(2-ethylhexyl)-2,3,4,5-tetrabromophthalate (Toronto Research Chemicals, Toronto, Ontario, Canada). Isopropylated triphenyl phosphate (IPTP) was a generous gift from W. Casey (National Institute of Environmental Health Sciences, National Institutes of Health in the United States). Analysis of the IPTP mixture was hampered by the lack of availability of pure standards for the various congeners suspected to be present. By comparing mass estimates of the whole molecules (from positive chemical ionization analyses) with those of molecular fragments (from electron impact mode analyses) we estimate that the majority of the material is composed of three congeners. These were triphenyl phosphate (TPP $\sim 18\%$); monoisopropylphenyl, diphenylphosphate (mITP $\sim 55\%$); and di(isopropylphenyl), phenylphosphate (dITP $\sim 25\%$). In addition, there was a small amount of tris(isopropylphenyl)phosphate present in the test material, but at a substantially lower concentration ($\sim 1.5\%$). Firemaster® 550 (FM550) was a generous gift from B. Chittam (Wellington Laboratories, Guelph, Ontario, Canada).

Culture and Differentiation of Human Primary Subcutaneous Preadipocytes

Primary human subcutaneous preadipocytes (ZenBio, Inc., Research Triangle Park, NC, USA) from female donors ages 25, 38, 40, 39, and 34 y with body mass indices of 18.8, 21.6, 23.3, 22.6, 21.5 (kg/m^2) and who were of several ethnicities (one Caucasian, two Hispanic, one Asian, and one unknown) were taken from thigh, back, abdomen, and flank depots and differentiated as previously described (Boucher et al. 2016) with modifications. Briefly, human primary preadipocytes were seeded in six-well dishes in subcutaneous preadipocyte media (PM-1, Zenbio Inc.), containing 10% fetal calf serum (Wisent, Montreal, Quebec, Canada). When cells reached confluence (day 0), they were treated with 100 nM insulin (I) and 500 μM IBMX (M) until day 4, with a media change on day 2. From day 4 onward, cells received insulin with media changes on days 4 and 8. For the positive control (MIDT), where the cells require both dexamethasone and troglitazone, dexamethasone (D) (1 μM) was added from days 0 to 14 and troglitazone (T) (5 μM) from days 2 to 14 in addition to MI. Treatments with the chemicals of interest were performed as follows: *a*) when the chemicals were tested for their ability to replace troglitazone, the cells were treated with dexamethasone from day 0 and the test chemical (0–200 μM FM550, 0–200 μM IPTP, 0–20 μM TPP, 0–20 μM TBPH, 0–20 μM TBB) from day 2, with media replacements on days 4 and 8 (MID condition); *b*) when the chemicals were to replace dexamethasone, the test chemical was added from day 0, and troglitazone with the test chemical were added from day 2 onward and replaced with media changes on days 2, 4, and 8 (MIT condition). IBMX and insulin were added in all treatments as described above for the MIDT condition.

Nile Red Staining of Lipids

Primary human preadipocytes were differentiated as described above for 14 d with the indicated treatments and controls in black collagen-coated 96-well plates (Fisher Scientific, Canada). The level of differentiation was assessed using a fluorescence plate reader as follows. At day 14, cells were fixed with 4% paraformaldehyde (VWR, Canada) for 30 min followed by PBS washes. Background fluorescence was read in PBS at 485/528 for Nile red and 360/460 for DAPI. Cells were then stained with Nile red (1 μg/mL) to stain for lipid droplets and DAPI (1 μg/mL) to stain nuclei as previously described (Greenspan et al. 1985). Nile red fluorescence was read at 485/528 nm (excitation/emission) in a Synergy 2 fluorescence plate reader (BioTek Instruments, Inc., Winooski, VT, USA) and DAPI staining, nuclei staining, was measured at 360/460 nm . To calculate Nile red to DAPI ratios the background fluorescence was first subtracted from the readings of Nile red and DAPI at the respective wavelengths, and Nile red/DAPI ratios were calculated for each of the wells.

Western Blotting

Human primary preadipocytes were seeded in six-well dishes and treated according to the differentiation protocol described above. On day 14, cells were lysed in RIPA buffer (20 mM Tris pH 7.5, 150 mM NaCl, 1 mM EDTA, 1% sodium deoxycholate, 2% NP-40, 0.4% SDS, 10% glycine) containing protease inhibitors (Roche Diagnostics, Laval, Quebec, Canada). Western blots were performed by probing with primary fatty acid binding protein (FABP) 4 and β-actin ACTB antibodies (Cell Signaling Technology, Danvers, MA, USA) followed by appropriate HRP-linked secondary antibodies, and developed using Clarity Western ECL Substrate (BioRad, Hercules, CA, USA). Relative optical densities were quantified using Image Lab software (BioRad), and values of terminal differentiation markers were normalized to ACTB levels.

mRNA Extraction and Real-Time Quantitative PCR (RT-qPCR)

Total RNA was extracted from differentiating human primary preadipocytes, treated as previously described. Samples were taken on days 4, 6, 9, and 12 using the RNeasy Mini kit and genomic DNA was eliminated using the RNase-Free DNase Kit (Qiagen, Mississauga, Ontario, Canada). RNA was reverse transcribed using iScript cDNA Synthesis Kit (BioRad). cDNA expression levels were analyzed by the CFX96-PCR Detection System using the iQSYBR SsoFast EvaGreen Supermix (BioRad). Primer sequences for each gene are summarized in Table S1. Primer efficiencies were $\geq 90\%$ and specificity was confirmed by sequence blast and melting curve analysis. All target gene transcripts were normalized to *ACTB* expression, which was not affected by treatment. Fold inductions were calculated using time-matched, control solvent-treated samples, and the comparative CT ($\Delta\Delta$CT) method was used for data analysis.

For RNA-seq analysis, total RNA was extracted from differentiating cells treated as described above using the RNeasy Kit and genomic DNA was eliminated using the RNase-Free DNase

Kit (both from Qiagen, Mississauga, Ontario, Canada). RNA was quantified and RNA quality was determined using a BioAnalyzer (Agilent Technologies, Santa Clara, CA, USA). RNA samples with A260/A280 ratios >1.8 and RNA integrity numbers (RIN) >8.0 were used.

Ion Proton™ Sequencing (RNA-Seq)

Total RNA from preadipocytes from five donors treated with MID, MITD, TPP, or IPTP was collected on day 6 of differentiation of preadipocytes, from five donors were used for RNA-Seq. Poly (A) RNA enrichment (DynaBeads® mRNA DIRECT Micro Kit, Thermo Fisher, Waltham, MA, USA) was performed for each sample on 1 μg of total RNA. The Ion Total RNA-Seq Kit version 2 (Thermo Fisher, Waltham, MA, USA) was used to fragment and prepare the sample libraries from poly (A)–enriched samples. The 3′-end barcode adapters provided in the Ion Xpress™ RNA-Seq Barcode Kit were ligated to the ends of the fragmented libraries (each PCR product receiving its own unique barcode). Libraries were then amplified using the Platinum® PCR SuperMix High Fidelity (Thermo Fisher, Waltham, MA, USA). Each amplified library was quantified/qualified using the High Sensitivity D1000 ScreenTape Kit and the Agilent® 2,200 TapeStation Instrument. Aliquots of each library were pooled together for a total final concentration of 50 pM. Emulsion PCR and chip loading was performed on the Ion Chef with the Ion P1 HI-Q Chef kit (Thermo Fisher, Waltham, MA, USA). The chips (P1 version 3) were run on the Ion Proton using the HI-Q chemistry. The Proton™ Torrent Server version 4.3 was used to interpret the sequencing data and generate unaligned binary version of a sequence aignment map (BAM) files for each barcoded sample. Reads were trimmed to remove low quality read prefixes, and then aligned to the reference genome (GRCh38v77) using Star (Dobin et al. 2013) and Bowtie (Langmead and Salzberg 2012). Following alignment, gene counting was performed with HT-Seq count (http://www-huber.embl.de/users/anders/HTSeq/doc/count.html) with the m parameter set to "intersection-nonempty" using the Ensembl GTF annotation (GRCh38v77). The table of counts was then imported into R (version 3.1.0; R Development Core Team) where genes that did not obtain a minimum total count of at least 0.5 reads per million within at least one dose group were removed from further analyses. The EdgeR (Robinson et al. 2010) package was used for the analysis. The data was normalized with TMM (Robinson and Oshlack 2010). The calculation of differentially expressed genes was performed using a paired design and using the GLM function. The data are publically available from Sequence Read Archive (http://www.ncbi.nlm.nih.gov/Traces/sra/sra.cgi?view=studies; BioProject ID SRP100037).

Biological and Pathway Analyses

All genes with a false discovery rate (FDR) $p < 0.05$ and fold change $> \pm 1.5$-fold compared with matched controls were considered DEGs and selected for further analyses. Biological functions, canonical pathways, and upstream regulatory molecules/networks were analyzed using Ingenuity Pathway Analysis (IPA) (Ingenuity Systems, Redwood City, CA, USA). DEGs were uploaded into IPA for functional analysis. Within IPA, a standard analytical workflow was used to identify the enriched canonical pathways, diseases, and biological functions, using adipose tissue as the target. The significance of the association between the gene expression data set and the pathways and functions in IPA was measured using IPA's built in Fischer's exact test (deemed significant if $p \leq 0.05$). (For further details see https://www.ingenuity.com/wp-content/themes/ingenuity-qiagen/pdf/ipa/IPA-netgen-algorithm-whitepaper.pdf).

Statistical Analyses

One-way ANOVA, followed by a Dunnett's or Tukey's post hoc test were used when comparing multiple means within an experiment. Student's *t*-test was used when comparing two means. Significance was defined as $p \leq 0.05$. Statistical analyses were performed using SigmaPlot software version 12.5 (San Jose, CA, USA) or GraphPad Prism version 7 (La Jolla, CA, USA).

Results

Effects of FM550, IPTP, and TPP on Adipogenesis in Human Primary Preadipocytes

Previous studies in murine cell models have shown that FM550, and its component TPP, increased adipogenesis through direct activation of PPARγ (Pillai et al. 2014). We investigated whether this is also true for human primary preadipocytes by assessing lipid accumulation and expression levels of adipogenic markers. Two conditions were used to establish whether FM550 and its components induce differentiation in human primary preadipocytes and if they act only through PPARG in this model system. One condition was a differentiation protocol where the chemicals of interest were added in the presence of IBMX, insulin, and dexamethasone (MID). The second condition was when the chemicals were added to human preadipocytes exposed to IBMX, insulin, and troglitazone (MIT). In positive controls, IBMX, insulin, dexamethasone, and troglitazone were added (MIDT).

Lipid accumulation was measured on day 14 by Nile red fluorescence values normalized to DAPI fluorescence. Human primary preadipocytes treated with the FM550 mixture exhibited a dose-dependent increase in lipid accumulation, with statistical significance achieved in the MID condition at 200 μM FM550, where a 4-fold increase as compared with MID alone was achieved (Figure 1A). TPP also induced a 4-fold increase in lipid accumulation relative to MID controls at 20 μM (Figure 1B). An increasing trend was also seen with TPP treatment in the MIT condition, but this was not statistically significant. IPTP treatment induced a significant ∼4-fold increase in lipid accumulation by Nile red staining at both 10 and 20 μM, as compared with the MID condition (Figure 1C). An increasing trend was also observed in the MIT condition; however, this increase did not reach statistical significance (Figure 1C). TBB and TBPH did not increase lipid accumulation, although an increasing trend was observed in the TBB dose–response curve (Figure 1D,E). As expected, the positive control MIDT increased lipid accumulation (see Figure S1).

Effects of FM550, IPTP, and TPP on FABP4 Protein Expression in the Presence of Dexamethasone

To further assess the extent of adipocyte differentiation and to delineate whether in human preadipocytes FM550 and its components up-regulate the expression of known PPARG targets, protein levels of the mature adipocyte marker, FABP4, were measured by Western blotting. In the presence of MID, 200 μM FM550 significantly increased FABP4 expression by ∼4-fold compared with MID controls; however, this effect was not observed when the mixture was added in the presence of MIT (Figure 2A). This may be partially due to the higher background in the presence of troglitazone given that FABP4 is a known target of PPARG. Similarly, 20 μM TPP induced a 6-fold increase in FABP4 expression relative to MID (Figure 2B), although increasing trends were observed at lower concentrations but did not reach statistical significance. Again, this effect was not observed in the presence of MIT (Figure 2B). Remarkably, IPTP treatment induced an increase not only at 20 μM (10-fold), but

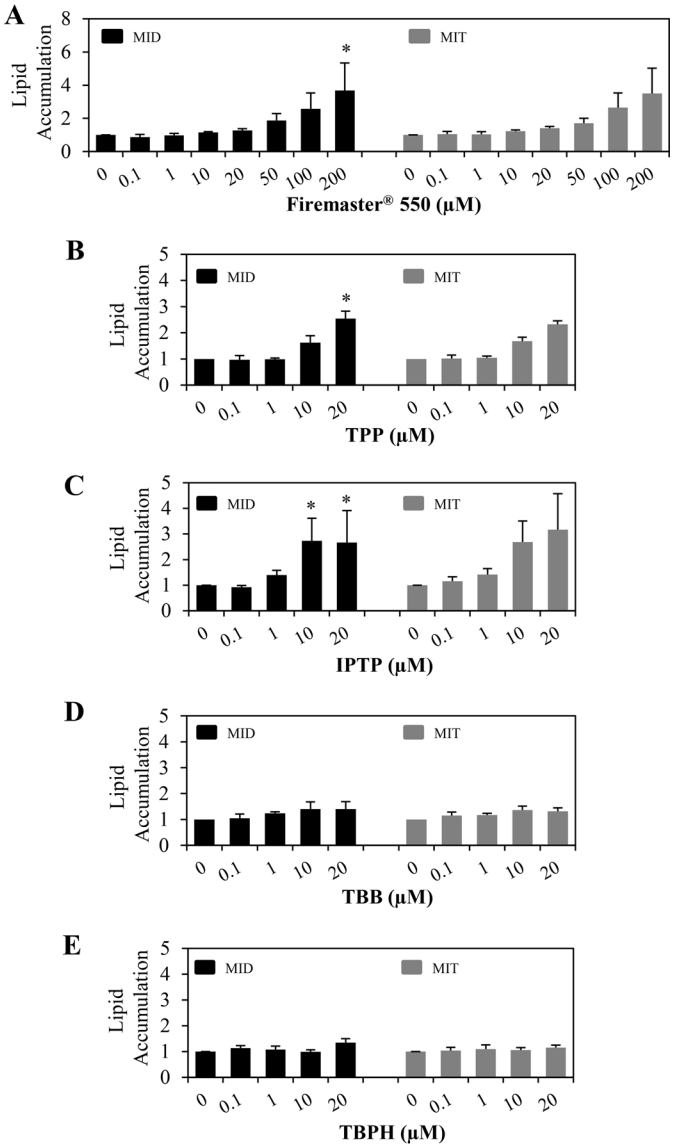

Figure 1. Effects of Firemaster 550®, and its components TPP and IPTP, on lipid accumulation in differentiating human preadipocytes. Human primary preadipocytes were induced to differentiate for 14 d in the presence of MI and 1 μM dexamethasone (MID) or MI and 5 μM troglitazone (MIT) supplemented with either FM550 (0–200 μM) or its components (TPP, IPTP, TBB, and TBPH; 0–20 μM). At day 14 of differentiation, lipid accumulation was quantified by Nile red staining normalized to DAPI. Data from all treatments, normalized to their respective control condition (MID or MIT), are graphically presented as mean ± SEM of four separate donor samples. *$p < 0.05$ compared with respective controls, as assessed by one-way ANOVA with Dunnett's post hoc tests.

also at 10 μM (5-fold) compared with MID controls (Figure 2C). Note that, at equivalent concentrations (10 and 20 μM), IPTP induced a higher expression of FABP4 relative to TPP treatment (Figure 2B,C). TBPH and TBB did not affect FABP4 protein expression in the presence of either MID or MIT (data not shown).

Effects of TPP and IPTP on the mRNA Expression of Transcriptional Regulators of Adipogenesis and Adipogenic Markers in Human Primary Preadipocytes

Our initial findings indicated that the MID condition was optimal for FM550-induced human adipocyte differentiation and that the FM550 components TPP and IPTP-containing 18% TPP were adipogenic. Therefore, the temporal changes in the mRNA levels of transcription factors and differentiation markers of adipogenesis were assessed in response to 20 μM TPP and 20 μM IPTP relative to MID controls.

First we assessed the mRNA levels of master regulators of adipogenesis, *PPARG* and CCAT enhancing binding protein α (*CEBPA*). *PPARG* expression was increased through the course of differentiation in TPP- and IPTP-treated cells relative to MID controls (Figure 3A). *CEBPA* levels were also increased following treatment with both TPP and IPTP during adipogenesis compared with MID controls (Figure 3B). In the TPP-treated cells, this increase was observed earlier in differentiation; however, similar levels were attained by both chemicals by the end of differentiation (Figure 3E). For the mature adipocyte markers, both *FABP4* and lipoprotein lipase (*LPL*) mRNA expression levels were increased with adipogenesis in response to both TPP and IPTP relative to MID control. Again, although the increase with IPTP was delayed relative to TPP, both components led to similar levels by the end of differentiation (Figure 3C, D). Perilipin (*PLIN*) mRNA expression, indicative of lipid droplet formation, was also up-regulated by TPP and IPTP during adipogenesis as compared with MID control. TPP increased *PLIN* levels as early as day 6, and the levels were maintained throughout the differentiation process. However, the increase by IPTP was to a lower extent than in TPP-treated cells and reached statistical significance only at day 9 (Figure 2E). We also measured the mRNA levels of the lipogenic transcription factor, sterol regulatory element binding transcription factor 1 (*SREBF1*), and found that both TPP and IPTP increased its expression during differentiation as compared with MID (Figure 3F). As expected, the positive control (i.e., MIDT) increased the expression of *PPARG*, *CEBPA*, *FABP4*, *LPL*, *PLIN*, and *SREBF1* throughout the differentiation process as illustrated in Figure S2.

Transcriptional Profiling of Human Primary Preadipocytes Treated with TPP, IPTP, and Troglitazone

To further investigate the effects of TPP and IPTP on the adipogenic pathway, human primary preadipocytes were differentiated in the presence of MID supplemented with 20 μM TPP, 20 μM IPTP, or 5 μM troglitazone. At day 6 of differentiation, RNA was collected from five donors and used for RNA-seq. Overall, TPP and IPTP treatments resulted in 380 and 713 DEGs, respectively, whereas troglitazone treatment resulted in 3,277 (Figure 4). Of the DEGs affected by TPP, only 5.8% were distinct; in contrast, 29% of DEGs affected by IPTP were unique. Most of the genes up-regulated by TPP (84%) were in common with troglitazone; whereas only 65% of the IPTP affected genes were also affected by troglitazone. Hierarchical cluster analysis of the fold changes for all DEGs from IPTP, troglitazone, and TPP shows that TPP- and IPTP-induced expression profiles cluster together and apart from troglitazone, indicating that they more closely resemble each other than the troglitazone-treatment group (Figure 4B). In addition, pairwise analysis using fold changes of the common genes shows that TPP-induced expression profiles are more strongly correlated with troglitazone and IPTP (correlation = 0.87 and 0.86, respectively), than IPTP is correlated with troglitazone (correlation = 0.75). All correlations are significant with a *p*-value of <0.00001. Overall, this analysis demonstrates that the DEGs in common across the treatments are highly correlated, and that IPTP is less similar to troglitazone than TPP. The top 10 up- and down-regulated DEGs affected by TPP, IPTP, and troglitazone are listed in Table 1. Table 1 shows that 45% of the top DEGs were common between TPP and IPTP, 20% of the top DEGs in TPP-treated cells were in common with troglitazone, and only 5% of the top DEGs in IPTP-treated cultures were in common with troglitazone.

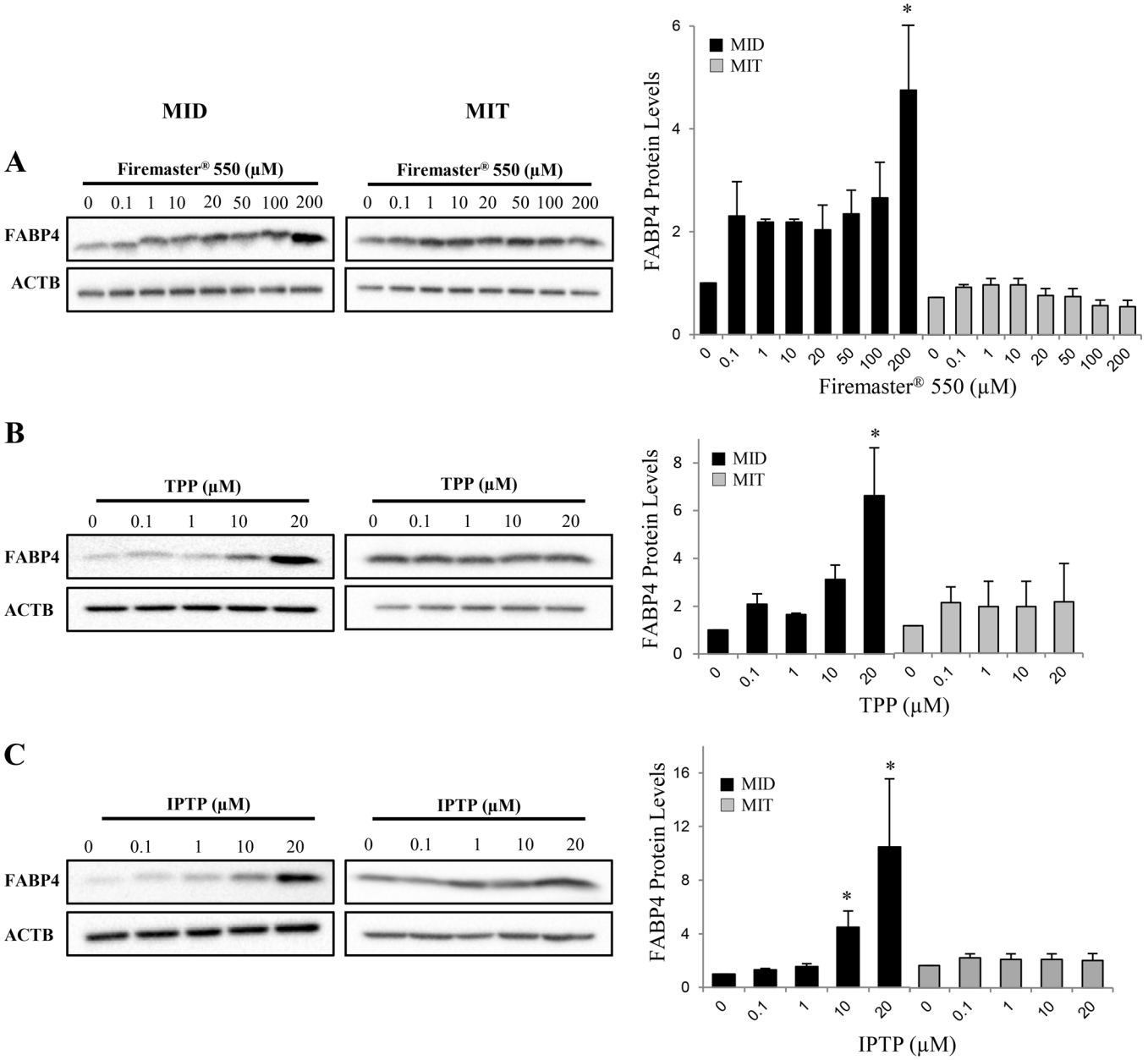

Figure 2. Effects of Firemaster 550®, and its components TPP and IPTP, on FABP4 protein expression in the presence of dexamethasone or troglitazone. Human primary preadipocytes were induced to differentiate for 14 d in the presence of MI and 1 μM dexamethasone (MID) or MI and 5 μM troglitazone (MIT) supplemented with either FM550 (0–200 μM) (*A*), or its components (TPP and IPTP; 0–20 μM) (*B*, *C*). Equal amounts of solubilized cellular proteins were separated by SDS-PAGE and immunoblotted with antibodies against FABP4 and ACTB as a loading control. Densitometric data from four separate donor samples, normalized to loading control, are graphically presented as means ± SEM. *$p < 0.05$ compared with respective controls, as assessed by one-way ANOVA with Dunnett's post hoc tests.

Validation of Select Differentially Expressed Genes by RT-qPCR

We validated some of the DEGs found in the RNA-seq analysis by RT-qPCR. Of the up-regulated genes, *FABP5*, *PLIN4*, and phosphoenolpyruvate carboxykinase 1 (*PCK1*) were increased in both TPP- and IPTP-treated cells. However, only TPP significantly increased the mRNA levels of the above genes (Figure 5A–C). By contrast, other genes including ATP-binding cassette subfamily G member 1 (*ABCG1*), solute carrier organic anion transporter family, member 4C1 (*SLCO4C1*), and *FABP3* were significantly increased by IPTP and not TPP (Figure 5D–F). It is possible that by adding more repeats we would have reached statistical significance for *FABP5*, *PCK1, PLIN4, ABCG1*, and *SLCO4C1* for both treatments. Some genes were equally increased by both treatments (Figure 5G–I). All of these genes were up-regulated by troglitazone control (see Figure S3). Interestingly, lipopolysaccharide binding protein (*LBP*) levels were down-regulated in IPTP-treated cells, not affected by TPP exposure, and up-regulated in troglitazone positive controls (Figure 5J; see also Figure S3). Further, keratin 18 (*KRT18*) levels were decreased by both TPP and IPTP; however, the expression of this gene was not changed in response to troglitazone (Figure 5K; see also Figure S3).

Canonical Pathways and Upstream Regulators Identified in IPA's Knowledge Base in Human Primary Preadipocytes Treated with TPP and IPTP

The DEGs obtained from the RNA-seq analysis of TPP, IPTP, and troglitazone treatments were analyzed using IPA to identify

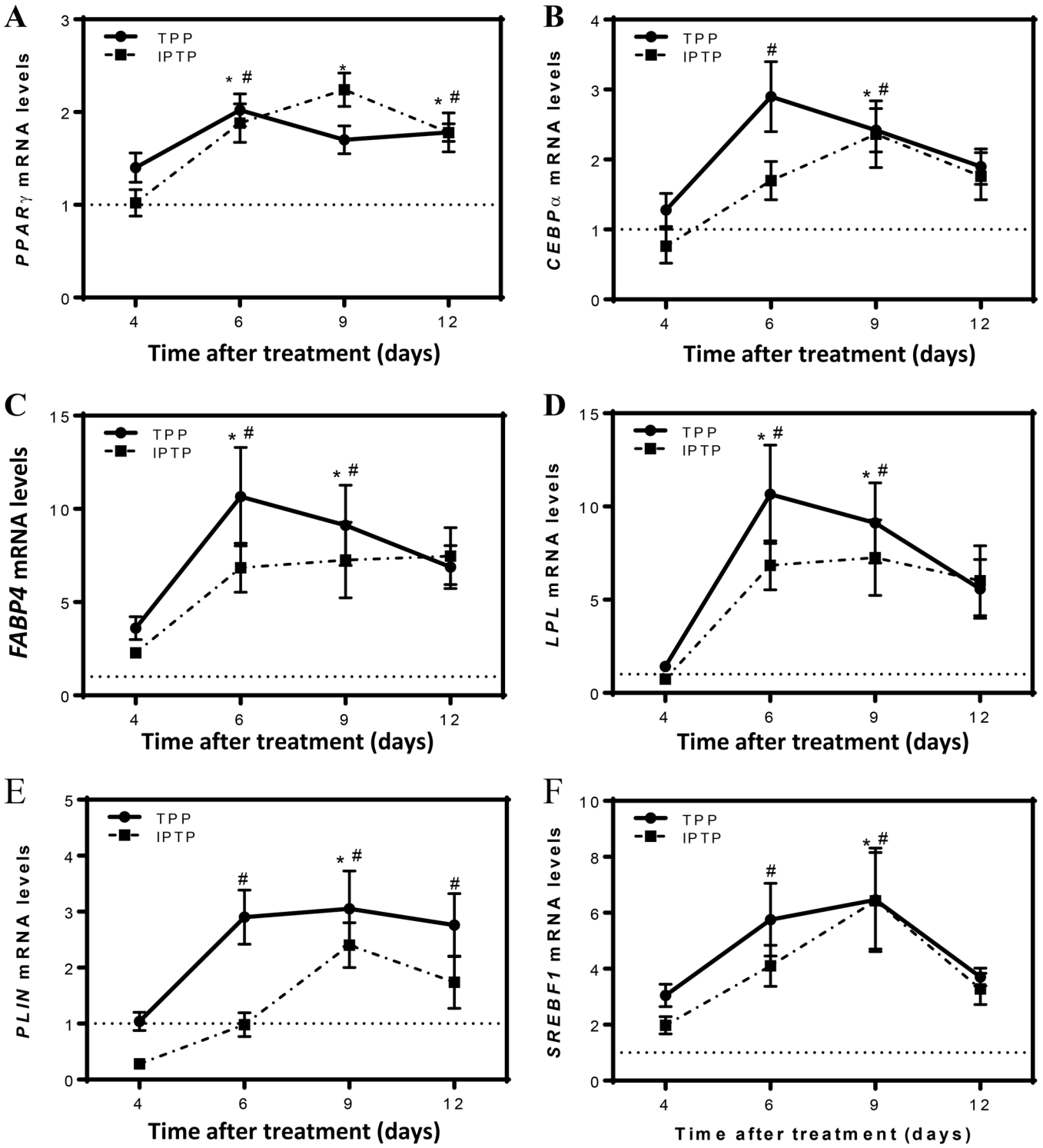

Figure 3. Effects of TPP and IPTP on the mRNA expression levels of transcriptional regulators of adipogenesis and adipogenic markers in differentiating human preadipocytes. Human primary preadipocytes were induced to differentiate for 4, 6, 9, and 12 d in the presence of 1 μM dexamethasone (MID) supplemented with either TPP (20 μM) or IPTP (20 μM). RNA was isolated and the mRNA levels of adipogenic markers, PPARG (*A*), CEBPA (*B*), FABP4 (*C*), LPL (*D*), PLIN1 (*E*), and SREBF1 (*F*) were quantified by real-time qPCR. Levels were normalized to endogenous ACTB mRNA, and expressed as a fold over the control condition (MID) for each time point. Results from five separate donor samples are graphically presented as means ± SEM. #$p < 0.05$ for TPP-treated cells, and *$p < 0.05$ for IPTP-treated cells compared with MID controls, as assessed by one-way ANOVA with Dunnett's post hoc tests.

enrichment of canonical pathways and upstream regulators. The top canonical pathways for each treatment identified in IPA are summarized in Table 2. As expected, the adipogenesis pathway was significantly enriched in TPP-, IPTP-, and troglitazone-treatment groups. In addition, there were several common pathways between TPP and IPTP treatments, such as liver X receptor (LXR)/retinoid X receptor (RXR) activation, cholesterol biosynthesis I, and lipopolyschariide (LPS)/interleukin-1 (IL-1)–mediated inhibition of RXR function (Table 2A,B). Of these pathways, only LPS/IL-1–mediated inhibition of RXR function

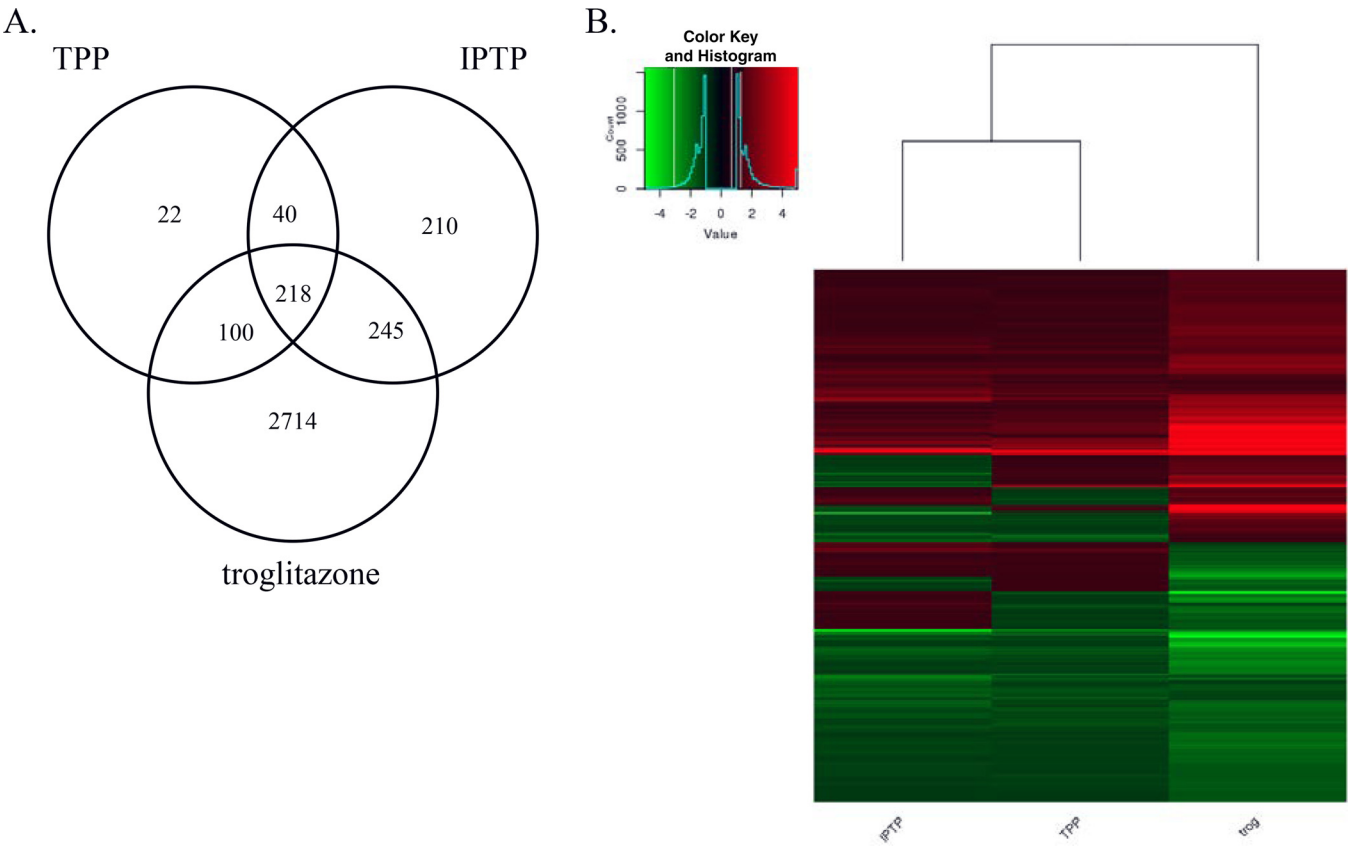

Figure 4. Differentially expressed genes (DEGs) affected by TPP, IPTP, and troglitazone. Human primary preadipocytes were differentiated in the presence of MID supplemented with 20 μM TPP, 20 μM IPTP, or 5 μM troglitazone. At day 6 of differentiation, RNA was collected from five donors and used for RNA-seq analysis. The overlap of significant ($-1.5 \leq$ fold change ≥ 1.5, FDR $p < 0.05$) DEGs between all treatments are depicted in a Venn diagram (*A*). Venn diagrams were produced using the on-line tool Venny (http://bioinfogp.cnb.csic.es/tools/venny/). (*B*) Hierarchical cluster analysis of the fold change for all DEGs from IPTP, troglitazone, TPP having an FDR of $p < 0.05$ and fold change >1.5. The distance is metric 1 − the Spearman correlation, values greater than 5 were truncated strictly for the color scale.

pathway was also in the top 20 pathways affected by troglitazone (Table 2C). Only 65% of the canonical pathways were common to both TPP and IPTP treatments. Some of the distinct pathways identified in TPP-treated cells were protein kinase A signaling, AMP-activated protein kinase (AMPK) signaling, and type II diabetes mellitus signaling. In the IPTP treatment, unique pathways included caveolar-mediated endocytosis signaling, clathrin-mediated endocytosis signaling, and acute phase response signaling. Of the top 20 pathways affected by IPTP and TPP treatment, several pathways overlapped and included superpathway of cholesterol biosynthesis, cholesterol biosynthesis (I, II, III), LXR/RXR activation (Table 2A,B). Troglitazone treatment was also associated with effects on pathways such as cAMP-mediated signaling and PXR/RXR activation, in addition to mitochondrial dysfunction and oxidative phosphorylation pathways (Table 2C).

Using IPA we also identified potential upstream regulators of the DEGs. As expected, PPARG was identified as a common top upstream regulator in an activated state for all treatments. In addition, SREBF1, another adipogenic transcriptional regulator, was found among the top upstream regulators. Accordingly, the insulin-induced gene (INSIG) 1 and 2, proteins known to be involved in the negative regulation of SREBF1 function, were predicted to be inhibited in all treatments. The membrane-bound transcription factor site-1 protease (MBTPS1) (also known as serine protease 1: S1P), a serine protease involved in SREBF1 activation, was predicted to be activated in all treatments as expected although not always in the top 20 (Inoue et al. 2001). By contrast, the transcription factor Krüppel-like factor (KLF) 15, known to be involved in adipocyte differentiation (Mori et al. 2005), was predicted to be active only in TPP and troglitazone treatments but not IPTP (Table 3). Furthermore, CEBPA, another important transcription factor in adipogenesis (Lane et al. 1996) was found as an upstream regulator in TPP and troglitazone treatments (not in the top 20), but not IPTP. Finally, lamin B1 (LMNB1), a matrix protein involved in cytoskeletal organization and adipogenesis (Verstraeten et al. 2011), was predicted to be inhibited by IPTP but not TPP or troglitazone treatment.

Using the common and unique DEGs to the three treatments identified by the Venn diagram (Figure 4) upstream regulators were identified in IPA. Table 4 shows the top upstream regulators using the common DEGs and Table 5 lists the upstream regulators based on the unique DEGs for TPP, IPTP, and troglitazone. As expected, PPARG was the top common upstream regulator for all treatments. Interestingly, based on the unique DEGs for TPP there were only few upstream regulators identified (Table 5A). IPTP had many more upstream regulators identified in IPA from which the top ones based on the number of molecules involved are being listed (Table 5B). As expected, troglitazone had the most upstream regulators identified in IPA based on a much larger number of unique DEGs, and the top 10 are listed in Table 5C.

Discussion

We found that FM550, and its components TPP and IPTP, induce adipogenesis in human primary preadipocytes as demonstrated

Table 1. Top 10 differentially expressed genes in differentiating human primary preadipocytes.

Gene symbol	Gene name	GO biological process	Fold change	FDR (*p*-value)
TPP				
ITIH1	Inter-alpha-trypsin inhibitor heavy chain 1	Hyaluronan metabolic process	7.9	<0.0001
PCK1	Phosphoenolpyruvate carboxykinase 1	Glucose metabolic process	7.1	<0.0001
FABP4	Fatty acid binding protein 4	Cholesterol homeostasis	6.6	<0.0001
GPBAR1	G-protein–coupled bile acid receptor 1	Cell surface bile acid receptor signaling pathway	5.7	<0.0001
PPP1R1A	Protein phosphatase 1 regulatory inhibitor subunit 1A	Glycogen metabolic process	5.6	<0.0001
SLCO4C1	Solute carrier organic anion transporter family, member 4C1	Cell differentiation	5.3	<0.0001
FNDC5	Fibronectin type III domain-containing protein 5	Response to muscle activity	4.6	<0.0001
ADIPOQ	Adiponectin, C1Q, and collagen domain containing	Adiponectin-activated signaling pathway	4.5	<0.0001
CDHR1	Cadherin-related family member 1	Homophilic cell adhesion via plasma membrane adhesion molecules	4.3	<0.0001
ITIH5	Inter-alpha (globulin) inhibitor H5	Negative regulation of peptidase activity	4.3	<0.0001
BPIFB4	BPI fold containing family B member 4	Lipid binding	−3.0	0.003
GPR78	G-protein–coupled receptor 78	Adenylate cyclase-activating G-protein–coupled receptor signaling pathway	−2.9	0.009
MYH11	Myosin heavy chain 11	Elastic fiber assembly	−2.6	0.0006
AMZ1	Archaelysin family metallopeptidase 1	Proteolysis	−2.5	<0.0001
FBXL22	F-box and leucine-rich repeat protein 22	Proteasome-mediated ubiquitin-dependent protein catabolic process	−2.4	<0.0001
RGS5	Regulator of G-protein signaling 5	Positive regulation of GTPase activity	−2.3	<0.0001
D4S234E	Neuron-specific gene family member 1	Positive regulation of receptor recycling	−2.3	0.0008
CORIN	Corin, serine peptidase	Peptide hormone processing	−2.2	<0.0001
KRT18	Keratin 18	Anatomical structure morphogenesis	−2.2	<0.0001
CNN1	Calponin 1	Actomyosin structure organization	−2.1	<0.0001
IPTP				
SLCO4C1	Solute carrier organic anion transporter family, member 4C1	Cell differentiation	7.9	<0.0001
TRIM63	Tripartite motif containing 63	Protein ubiquitination	6	<0.0001
ABCG1	ATP-binding cassette subfamily G member 1	Cholesterol metabolic process	5.9	<0.0001
ITIH1	Inter-alpha-trypsin inhibitor heavy chain 1	Hyaluronan metabolic process	5.7	<0.0001
FABP3	Fatty acid binding protein 3	Fatty acid metabolic process	4.8	<0.0001
FNDC5	Fibronectin type III domain containing 5	Response to muscle activity	4.9	<0.0001
PLEKHG6	Pleckstrin homology and RhoGEF domain containing G6	Positive regulation of GTPase activity	4.7	<0.0001
RNF157	Ring finger protein 157	Zinc ion binding	4.6	<0.0001
EFNA1	Ephrin A1	Activation of MAPK activity	4.6	<0.0001
PPP1R1A	Protein phosphatase 1 regulatory inhibitor subunit 1A	Glycogen metabolic process	4.2	<0.0001
MYH11	Myosin heavy chain 11	Elastic fiber assembly	−4.8	<0.0001
LBP	Lipopolysaccharide binding protein	Lipopolysaccharide-mediated signaling pathway	−4.5	<0.0001
RGS5	Regulator of G-protein signaling 5	Positive regulation of GTPase activity	−4.5	<0.0001
OXTR	Oxytocin receptor	G-protein–coupled receptor signaling pathway	−4.1	<0.0001
KRT18	Keratin 18	Anatomical structure morphogenesis	−3.7	<0.0001
DKK2	Dickkopf WNT signaling pathway inhibitor 2	Wnt signaling pathway	−3.6	<0.0001
FBXL22	F-box and leucine-rich repeat protein 22	Proteasome-mediated ubiquitin-dependent protein catabolic process	−3.5	<0.0001
CXCL5	C-X-C motif chemokine ligand 5	G-protein–coupled receptor signaling pathway	−3.4	<0.0001
CORIN	Corin, serine peptidase	Peptide hormone processing	−3.4	<0.0001
TLL1	Tolloid like 1	Cell differentiation	−3.2	<0.0001
Troglitazone				
SCN4A	Sodium voltage-gated channel alpha subunit 4	Regulation of ion transmembrane transport	261.5	<0.0001
CD96	CD96 molecule	Cell adhesion	147.7	<0.0001
PCK1	Phosphoenolpyruvate Carboxykinase 1	Glucose metabolic process	121.3	<0.0001
ADAMTS18	ADAM metallopeptidase with thrombospondin type 1 motif 18	Proteolysis	113.0	<0.0001
MOGAT1	Monoacylglycerol O-acyltransferase 1	Diacylglycerol biosynthetic process	107.2	<0.0001
ADRA1A	Adrenoceptor alpha 1A	G-protein–coupled receptor signaling pathway	98.3	<0.0001
SCGN	Secretagogin, EF-hand calcium binding protein	Regulation of cytosolic calcium ion concentration	93.3	<0.0001
PPP1R1A	Protein phosphatase 1 regulatory inhibitor subunit 1A	Glycogen metabolic process	67.8	<0.0001

Table 1. (*Continued*.)

Gene symbol	Gene name	GO biological process	Fold change	FDR (*p*-value)
CDH22	Cadherin 22	Calcium-dependent cell-cell adhesion via plasma membrane cell adhesion molecules	61.6	<0.0001
ADIPOQ	Adiponectin, C1Q, and collagen domain containing	Adiponectin-activated signaling pathway	56.6	<0.0001
CCL13	C-C motif chemokine ligand 13	G-protein–coupled receptor signaling pathway	−9.8	<0.0001
STEAP4	STEAP4 metalloreductase	Iron ion homeostasis	−6.7	<0.0001
PPP2R2C	Protein phosphatase 2 regulatory subunit Bgamma	Regulation of protein phosphatase type 2A activity	−6.1	<0.0001
PMAIP1	Phorbol-12-myristate-13-acetate-induced protein 1	Intrinsic apoptotic signaling pathway	−6.1	<0.0001
BPIFB4	BPI fold containing family B member 4	Lipid binding	−6.1	<0.0001
CSF3	Colony stimulating factor 3	Cellular response to cytokine stimulus	−5.9	<0.0001
RAB27B	RAB27B, member RAS oncogene family	Small GTPase-mediated signal transduction	−5.9	<0.0001
WISP1	WNT1 inducible signaling pathway protein 1	Wnt signaling pathway	−5.8	<0.0001
FRMPD4	FERM and PDZ domain containing 4	Positive regulation of synapse structural plasticity	−5.4	<0.0001
RGCC	Regulator of cell cycle	Fibroblast activation	−5.2	<0.0001

Note: Human primary preadipocytes were differentiated in the presence of MID supplemented with 20 μM TPP, 20 μM IPTP, or 5 μM troglitazone. At day 6 of differentiation, RNA was collected from five donors and used for RNA-seq analysis. The top 10 up- and down-regulated genes are shown. FDR, false discovery rate; GO, gene ontology.

by lipid accumulation and expression of adipogenic markers. Further, we found that IPTP was able to increase lipid accumulation and FABP4 protein expression at lower concentrations than TPP. Our findings are in agreement with a previous study showing that treatment of murine pluripotent cells with the FM550 components TPP and IPTP diverted the cells to an adipogenic fate, as assessed by lipid accumulation and perilipin levels (Pillai et al. 2014). However, (Pillai et al. 2014) used an IPTP mixture containing 40% TPP and concluded that the main adipogenic component in FM550 was likely TPP. Here we show in human primary preadipocytes that an IPTP mixture containing only 18% TPP was more potent than pure TPP at inducing lipid accumulation and FABP4 expression.

The human preadipocyte differentiation model system allowed us to explore the mode of action of the chemicals of interest leading to adipogenesis and, potentially, obesity whether through PPARG activation or glucocorticoid pathways. Chemicals are tested for their ability to activate PPARG when replacing troglitazone in the differentiation medium and via the glucocorticoid pathway when chemicals are replacing dexamethasone. FM550 and its components, TPP and IPTP, are able to increase lipid accumulation in the presence of dexamethasone in human preadipocytes, although a positive trend, which did not reach statistical significance, was also observed in the presence of troglitazone for this end point in our study. It is very likely that statistical significance would have been achieved if more donors were used for the experiments. Using a murine model, others have shown that TPP and IPTP increased lipid accumulation; however, it is unclear which nuclear receptor these chemicals are targeting because murine cell models require either dexamethasone or troglitazone for differentiation (Gimble et al. 1990). Our lipid accumulation data suggest that FM550, TPP, and IPTP may have other effects in addition to PPARG activation. Further, we have shown that in the murine 3T3-L1 model, the lipogenesis (lipid accumulation) mediated by dexamethasone TPP and IPTP was not inhibited by the PPARG antagonist GW9662, whereas troglitazone-mediated lipogenesis was (Tung et al. 2017). Moreover, in our study the test chemicals were added in the presence of 5 μM troglitazone, a concentration by which PPARG is likely to be saturated (Nagai et al. 2011) and unlikely to be further activated, supporting that mechanisms beyond PPARG activation are at work for lipogenesis. Therefore one may hypothesize that the glucocorticoid receptor may be a target. However, TPP and IPTP were not able to activate the glucocorticoid receptor in luciferase reporter assays (data not shown). Of further note, Pillai et al. (2014) showed a modest increase in PPAR transactivation by TPP and IPTP relative to solvent control, and also showed that TPP was more potent than IPTP in mediating this effect. Therefore, these authors concluded that TPP was the adipogenic component in FM550 (Pillai et al. 2014). Interestingly, we observed a higher PPARG transactivation in IPTP treatments compared with TPP treatments in luciferase assays (data not shown). Of importance, our mixture of isopropylated compounds (IPTP) contained only 18% TPP by analysis, whereas Pillai et al. (2014) used a mixture containing 40%. Therefore, one may not conclude that TPP is the main PPARG activator in the FM550 mixture or that this is the only mechanism of action of the chemicals.

In addition to using a human model to assess the effects of FM550 components in inducing adipogenesis, we also performed global gene expression analysis to evaluate the mode of action of these chemicals. To the best of our knowledge, this study is the first to compare global transcriptomic changes in response to FM550 components in differentiating human preadipocyte or any other system. Interestingly, we found that IPTP treatment resulted in twice the number of affected DEGs as TPP. About half of the

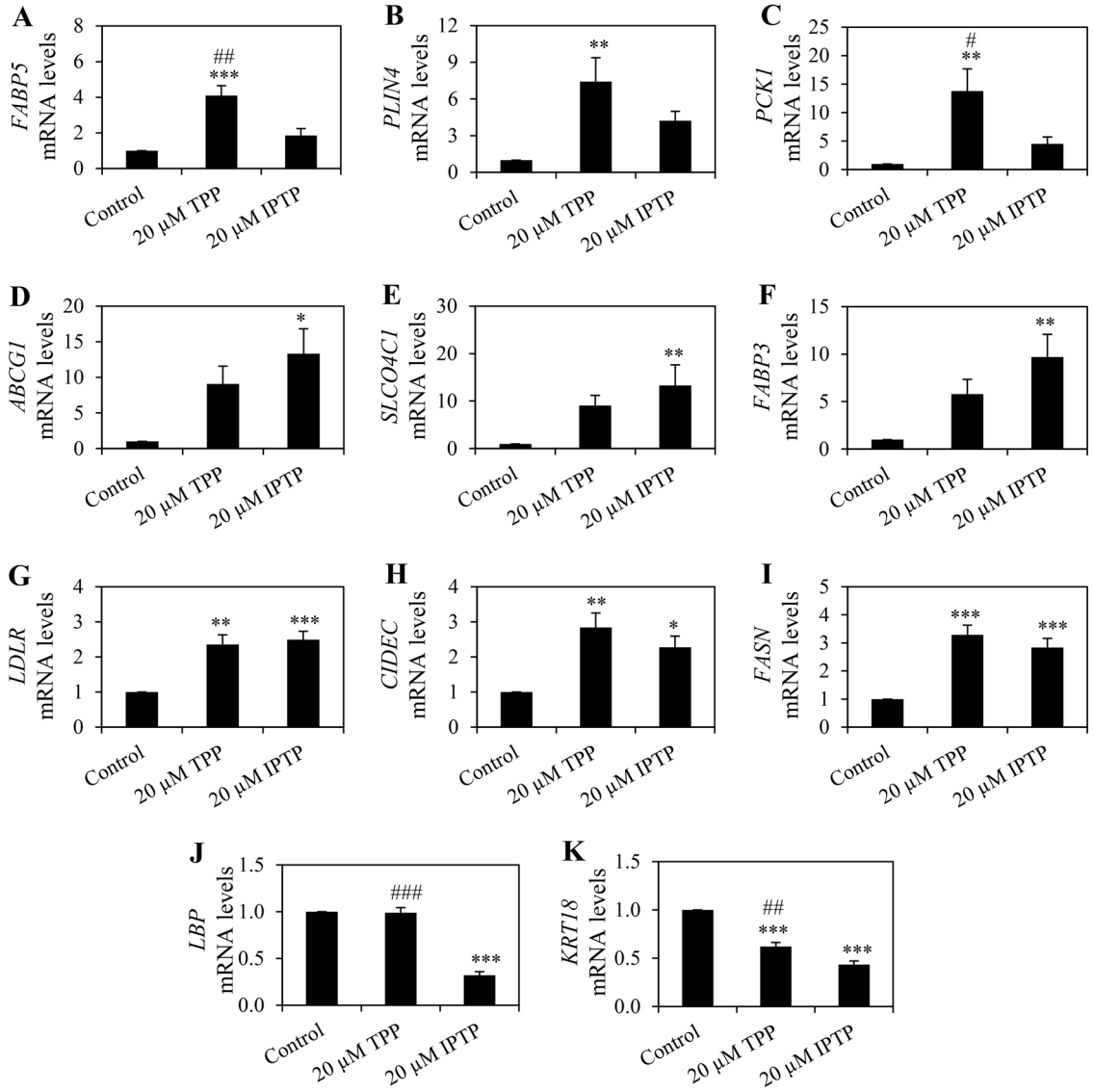

Figure 5. Validation of selected differentially expressed genes (DEGs) by RT-qPCR. Human primary preadipocytes were differentiated in the presence of MID supplemented with 20 μM TPP or 20 μM IPTP. At day 6 of differentiation, RNA was collected for RNA-seq analysis. The mRNA levels of select DEGs from RNA-seq analysis were quantified by RT-qPCR. Levels were normalized to endogenous ACTB mRNA, and expressed as a fold over the control condition (MID) for each treatment. Results from five separate donor samples are graphically presented as means ± SEM. $*p < 0.05$, $**p < 0.01$, and $***p < 0.001$ for TPP- and IPTP- treated samples compared with control; $\#p < 0.05$, $\#\#p < 0.01$, and $\#\#\#p < 0.001$ for TPP-treated compared with IPTP-treated samples, as assessed by one-way ANOVA with Tukey's post hoc tests.

DEGs affected by IPTP were distinct (i.e., were not shared with either TPP or troglitazone). In contrast, most of the TPP-affected DEGs were in common with troglitazone treatment. This suggests that TPP acts mainly through PPARG activation, whereas IPTP perturbed a variety of regulatory pathways beyond just PPARG. Indeed, ~84% of the DEGs induced by TPP treatment were in common with DEGs induced by the PPARG agonist troglitazone, as opposed to 64% DEGs in common between IPTP and troglitazone.

When we assessed the transcript levels of select DEGs by RT-qPCR, we found striking differences between the three treatments. The fold change in the expression of some DEGs was larger in the TPP treatment versus the IPTP treatment, and *vice versa*. For example, *PCK1*, *PLIN4*, and *FABP5* were all increased to a greater extent by TPP. All these genes are involved in lipogenesis, an integral part of adipocyte differentiation (Ducharme and Bickel 2008). Interestingly, IPTP treatment induced higher expression levels of transporters, such as *ABCG1* and *SLCO4C1* than TPP. ABCG1 expression is positively correlated with triglyceride accumulation during adipogenesis by increasing fatty acid influx (Frisdal et al. 2015). Fatty acids are known to act as endogenous PPARG agonists (Krey et al. 1997), and therefore this may be a plausible mechanism by which these chemicals indirectly activate PPARG. SLCO4C1 is a member of the transporter superfamily mediating the transport of thyroid hormones, T_3 and T_4 (van der Deure et al. 2010). It has been shown that when preadipocytes are transduced with an inactive thyroid hormone receptor mutant a decrease in the expression of adipogenic markers is observed (Liu et al. 2015). This suggests that increased intracellular thyroid hormone levels, which may be mediated by SLCO4C1, enhance human adipogenesis.

The distinct effects observed in the TPP and IPTP treatments are also apparent in the canonical pathways enriched in IPA. For TPP treatment, many of the pathways were in common with the troglitazone treatment, as expected, although some were unique. Of those, protein kinase A signaling is relevant, as it is elevated

Table 2. Top 20 significant canonical pathways identified by IPA.

IPA canonical pathway	*p*-Value	Ratio
TPP		
LXR/RXR activation	<0.0001	0.227
LPS/IL-1–mediated inhibition of RXR function	<0.0001	0.109
Superpathway of cholesterol biosynthesis	<0.0001	0.688
TR/RXR activation	<0.0001	0.177
Protein kinase A signaling	0.009	0.0526
Tight junction signaling	0.0002	0.0909
AMPK signaling	0.001	0.0758
Adipogenesis pathway	0.0003	0.0947
Hepatic fibrosis/hepatic stellate cell activation	0.001	0.0796
ILK signaling	0.002	0.0769
Cholesterol biosynthesis I	<0.0001	0.889
Cholesterol biosynthesis II (via 24,25-dihydrolanosterol)	<0.0001	0.889
Cholesterol biosynthesis III (via Desmosterol)	<0.0001	0.889
Cellular effects of sildenafil (Viagra)	<0.0001	0.133
Type II diabetes mellitus signaling	0.0008	0.093
G-protein–coupled receptor signaling	0.019	0.0552
Cardiac β-adrenergic signaling	0.001	0.0972
cAMP-mediated signaling	0.01	0.0631
Stearate biosynthesis I (animals)	<0.0001	0.231
FXR/RXR activation	0.003	0.0968
IPTP		
LXR/RXR activation	<0.0001	0.288
Hepatic fibrosis/hepatic stellate cell activation	<0.0001	0.159
LPS/IL-1–mediated inhibition of RXR function	<0.0001	0.124
Clathrin-mediated endocytosis signaling	0.003	0.0917
Superpathway of cholesterol biosynthesis	<0.0001	0.625
Acute phase response signaling	0.003	0.0962
Tight junction signaling	0.005	0.0909
ILK signaling	0.008	0.0855
FXR/RXR activation	0.0003	0.145
TR/RXR activation	0.0003	0.145
Agranulocyte adhesion and diapedesis	0.005	0.0978
Cellular effects of sildenafil (Viagra)	0.001	0.133
Cholesterol biosynthesis I	<0.0001	0.778
Cholesterol biosynthesis II (via 24,25-dihydrolanosterol)	<0.0001	0.778
Cholesterol biosynthesis III (via Desmosterol)	<0.0001	0.778
Atherosclerosis signaling	0.01	0.101
Hepatic cholestasis	0.04	0.0761
Adipogenesis pathway	0.05	0.0737
Caveolar-mediated endocytosis signaling	0.008	0.118
Paxillin signaling	0.03	0.0896
Troglitazone		
Role of macrophages, fibroblasts, and endothelial cells in rheumatoid arthritis	0.017	0.236
Mitochondrial dysfunction	<0.0001	0.425
Noradrenaline and adrenaline degradation	0.001	0.5
Mitochondrial L-carnitine shuttle pathway	0.005	0.545
LPS/IL-1–mediated inhibition of RXR function	<0.0001	0.38
cAMP-mediated signaling	0.003	0.279
Fatty acid β-oxidation I	<0.0001	0.625
Cardiac β-adrenergic signaling	0.001	0.319
PXR/RXR activation	0.028	0.295
Agranulocyte adhesion and diapedesis	0.019	0.261
Melanocyte development and pigmentation signaling	0.005	0.316
Glutaryl-CoA degradation	<0.0001	0.9
PPARα/RXRα activation	<0.0001	0.316
p38 MAPK signaling	0.011	0.295
Sperm motility	0.011	0.295
Oleate biosynthesis II (animals)	0.019	0.571
Endothelin-1 signaling	0.028	0.25
Myc-mediated apoptosis signaling	0.039	0.289
Regulation of the epithelial–mesenchymal transition pathway	0.02	0.252
Glutathione-mediated detoxification	0.017	0.412

Note: Human primary preadipocytes were differentiated in the presence of MID supplemented with 20 μM TPP, 20 μM IPTP, or 5 μM troglitazone. At day 6 of differentiation, RNA was collected from five donors and used for RNA-seq. Genes that had $\geq +1.5$ or ≤ -1.5 a fold change were uploaded in to IPA for analysis using the adipose tissue as the target organ. The pathways were sorted by number of molecules involved and the top 20 are shown.

early in adipogenesis (Klemm et al. 1998). During a standard differentiation protocol, IBMX is used to increase intracellular cAMP concentrations, which in turn activates PKA (Reusch et al. 2000). Because all treatments contained IBMX, a phosphodiesterase inhibitor, it is remarkable that only TPP further increased this process. Another relevant pathway that was enriched in TPP

Table 3. Top 20 upstream regulators identified by IPA.

Upstream regulator	Molecule type	Predicted activation state	Activation *z*-score	*p*-Value
TPP				
PPARG	Ligand-dependent nuclear receptor	Activated	5.895	<0.0001
SREBF1	Transcription regulator	Activated	5.424	<0.0001
SCAP	Other	Activated	4.618	<0.0001
CEBPA	Transcription regulator	Activated	3.652	<0.0001
NR1H3	Ligand-dependent nuclear receptor	Activated	3.546	<0.0001
PPARGC1A	Transcription regulator	Activated	3.465	<0.0001
ATP7B	Transporter	Activated	3.464	<0.0001
PPARGC1B	Transcription regulator	Activated	3.248	<0.0001
KLF15	Transcription regulator	Activated	2.905	<0.0001
NR1H2	Ligand-dependent nuclear receptor	Activated	2.865	<0.0001
INSIG1	Other	Inhibited	−4.967	<0.0001
POR	Enzyme	Inhibited	−3.069	<0.0001
ELOVL5	Enzyme	Inhibited	−2.976	<0.0001
EPAS1	Transcription regulator	Inhibited	−2.969	<0.0001
INSIG2	Other	Inhibited	−2.934	<0.0001
ASXL1	Transcription regulator	Inhibited	−2.646	<0.0001
TNF	Cytokine	Inhibited	−2.620	<0.0001
MKL1	Transcription regulator	Inhibited	−2.591	<0.0001
LEP	Growth factor	Inhibited	−2.480	<0.0001
PML	Transcription regulator	Inhibited	−2.462	<0.0001
IPTP				
SREBF1	Transcription regulator	Activated	4.43	<0.0001
PPARG	Ligand-dependent nuclear receptor	Activated	4.20	<0.0001
SCAP	Other	Activated	4.05	<0.0001
NR1H3	Ligand-dependent nuclear receptor	Activated	3.70	<0.0001
ATP7B	Transporter	Activated	3.32	<0.0001
PPARGC1B	Transcription regulator	Activated	2.93	<0.0001
MBTPS1	Peptidase	Activated	2.43	<0.0001
PPARD	Ligand-dependent nuclear receptor	Activated	2.38	<0.0001
FAS	Transmembrane receptor	Activated	2.35	<0.0001
NR1H2	Ligand-dependent nuclear receptor	Activated	2.23	<0.0001
INSIG1	Other	Inhibited	−4.64	<0.0001
EPAS1	Transcription regulator	Inhibited	−3.08	<0.0001
ELOVL5	Enzyme	Inhibited	−2.98	<0.0001
MKL1	Transcription regulator	Inhibited	−2.94	<0.0001
IKBKB	Kinase	Inhibited	−2.84	<0.0001
TGFB1	Growth factor	Inhibited	−2.83	<0.0001
INSIG2	Other	Inhibited	−2.76	<0.0001
POR	Enzyme	Inhibited	−2.75	<0.0001
LEP	Growth factor	Inhibited	−2.48	<0.0001
LMNB1	Other	Inhibited	−2.43	<0.0001
Troglitazone				
PPARG	Ligand-dependent nuclear receptor	Activated	6.706	<0.0001
PPARA	Ligand-dependent nuclear receptor	Activated	6.302	<0.0001
PPARGC1A	Transcription regulator	Activated	6.283	<0.0001
SREBF1	Transcription regulator	Activated	5.048	<0.0001
SCAP	Other	Activated	4.942	<0.0001
RB1	Transcription regulator	Activated	4.767	<0.0001
KLF15	Transcription regulator	Activated	4.712	<0.0001
INSR	Kinase	Activated	4.667	<0.0001
PPARGC1B	Transcription regulator	Activated	4.223	<0.0001
PNPLA2	Enzyme	Activated	3.763	<0.0001
RICTOR	Other	Inhibited	−5.182	<0.0001
INSIG1	Other	Inhibited	−5.099	<0.0001
TNF	Cytokine	Inhibited	−4.972	<0.0001
KDM5A	Transcription regulator	Inhibited	−4.494	<0.0001
TWIST1	Transcription regulator	Inhibited	−3.656	<0.0001
F2R	G-protein–coupled receptor	Inhibited	−3.359	<0.0001
TGFB1	Growth factor	Inhibited	−3.189	<0.0001
INSIG2	Other	Inhibited	−3.088	<0.0001
Aldosterone	Chemical–endogenous mammalian	Inhibited	−3.084	<0.0001
HSD17B4	Enzyme	Inhibited	−2.985	<0.0001

Note: Human primary preadipocytes were differentiated in the presence of MID supplemented with 20 μM TPP, 20 μM IPTP, or 5 μM troglitazone. At day 6 of differentiation, RNA was collected from five donors and used for RNA-seq. Genes that had $\geq +1.5$ or ≤ -1.5 a fold change were uploaded into IPA for analysis using the adipose tissue as the target organ. The upstream regulators were sorted by *z*-score and the top 20 are shown.

treatment was AMPK Signaling, which is involved in energy metabolism and fatty acid oxidation (Hardie et al. 2006). Some of the IPTP perturbed pathways included caveolar-mediated endocytosis signaling and clathrin-mediated endocytosis signaling, both of which are involved in insulin receptor and solute carrier family 2 (facilitated glucose transporter), member 4

Table 4. Top upstream regulators identified by IPA for TPP, IPTP, and troglitazone overlapping DEGs.

Upstream regulator	Molecule type	*p*-Value
TPP, IPTP, MIDT		
PPARG	Ligand-dependent nuclear receptor	<0.001
NR1H2	Ligand-dependent nuclear receptor	<0.001
GHRL	Growth factor	<0.001
Dihydrotestosterone	Chemical–endogenous mammalian	<0.001
FGF21	Growth factor	<0.001
LEP	Growth factor	<0.001
NR4A1	Ligand-dependent nuclear receptor	<0.001
TNF	Cytokine	<0.001

Note: Human primary preadipocytes were differentiated in the presence of MID supplemented with 20 μM TPP, 20 μM IPTP or 5 μM troglitazone. At day 6 of differentiation, RNA was collected from five donors and used for RNA-seq. Genes that had $\geq +1.5$ or ≤ -1.5 a fold change were uploaded into Venny version 2.0 for analysis and overlapping DEGs were uploaded into IPA. Only pathways containing more than five molecules are shown.

Table 5. Top upstream regulators identified by IPA using unique DEGs to TPP, IPTP, and troglitazone.

Upstream regulator	Molecule type	*p*-Value
TPP		
DICER1	Enzyme	<0.0001
miR-7155-5p (miRNAs w/seed CUGGGGU)	Mature microRNA	<0.0001
miR-4667-5p (and other miRNAs w/seed CUGGGGA)	Mature microRNA	<0.0001
IPTP		
beta-Estradiol	Chemical–endogenous mammalian	<0.002
Lipopolysaccharide	Chemical drug	<0.002
Dexamethasone	Chemical drug	<0.002
TNF	Cytokine	<0.002
TGFB1	Growth factor	<0.002
IFNG	Cytokine	<0.002
ESR1	Ligand-dependent nuclear receptor	<0.002
TP53	Transcription regulator	<0.002
IL1B	cytokine	<0.002
Troglitazone		
TP53	Transcription regulator	<0.0001
ERBB2	Kinase	<0.0001
CCND1	Transcription regulator	<0.0001
TGFB1	Growth factor	<0.0001
RB1	Transcription regulator	<0.0001
E2F4	Transcription regulator	<0.0001
CDKN1A	Kinase	<0.0001
NUPR1	Transcription regulator	<0.0001
calcitriol	Chemical drug	<0.0001
Vegf	Group	<0.0001

Note: Human primary preadipocytes were differentiated in the presence of MID supplemented with 20 μM TPP, 20 μM IPTP or 5 μM troglitazone. At day 6 of differentiation, RNA was collected from five donors and used for RNA-seq. Genes that had $\geq +1.5$ or ≤ -1.5 a fold change were uploaded into Venny version 2.0 for analysis and unique genes for TPP, IPTP, and troglitazone were uploaded into IPA. Data were sorted by number of molecules per pathway and only pathways containing more than three molecules for TPP and five molecules for IPTP and troglitazone are shown.

(GLUT4) endocytosis, respectively (Fagerholm et al. 2009; Leto and Saltiel 2012). In addition, IPTP also affected the paxillin signaling pathway, which is involved in cytoskeletal remodeling, an important process in adipocyte differentiation (Kawaguchi et al. 2003; Parsons et al. 2012). This further indicates that although both chemicals may modulate adipogenesis, their modes of action may be different.

The top upstream regulators identified by IPA for all treatments are known regulators of the adipogenic process. With respect to these identified regulators, the mode of action of TPP appears to resemble the mode of action of troglitazone. In addition, the few upstream regulators that were identified in IPA using the unique DEGs to TPP did not appear to have any known function in adipogenesis. However, for IPTP dexamethasone was identified as one of the top upstream regulators using unique DEGs. Of note, CEBPA, an important transcription factor in adipogenesis was identified as an upstream regulator in TPP and troglitazone-treated cells (not in the top 10) but not in IPTP. In addition, CEBPA was not a DEG identified in the IPTP treatment; however, this may be due to the delayed increase in mRNA expression of CEBPA by IPTP treatment, which reached significance only at day 9 (Figure 3). This is not surprising considering that the mRNA used in the RNA-seq analysis was obtained at an earlier time point (day 6). This is one limitation of this study, where we chose one most potent concentration and one time point to generate the data due to prohibiting costs. Further, the concentration of FM550 and its components used in this study were in the μM range, whereas human exposure is estimated at the nM range. However, it is difficult to extrapolate *in vitro* doses to human exposure. First, human exposure is chronic and some of the chemicals may have lipophilic properties and may be accumulative in tissues, including the fat tissue. In fact, accumulation of FM550 components was detected in the blubber of some marine species, showing that these compounds may accumulate in adipose tissue (Lam et al. 2009). In addition, chemicals may adhere to the plastic or media components *in vitro*, and therefore the intracellular concentrations may be different than the ones applied. More knowledge is needed on the pharmacokinetics of FM550 and its components in humans and in cell culture in order to be able to model how the doses used *in vitro* correlate to the *in vivo* exposure. Future studies will focus on DEGs of interest to establish the mode of action of TPP and IPTP in more depth.

Conclusion

In conclusion, we demonstrated that FM550 and its components, TPP and IPTP, induced adipogenesis in human primary preadipocytes *in vitro*. Although others have concluded that TPP is the main adipogenic component in FM550 and an activator of PPARG in a murine model system, using the human model we show that IPTP is also adipogenic. Global gene expression profiles revealed that both components had a gene signature that supported an adipogenic end point. However, of the two, TPP seemed to have a mode of action more similar to that of a known PPARG agonist. Interestingly, IPTP exhibited a more distinct gene profile from the PPARG agonist. Taken together, we show that although both components of FM550 increase human adipocyte differentiation, they may also exert other effects via different mechanisms. Overall, the results of this study suggest that human exposure to FM550 may promote adverse metabolic effects and as such, further investigation into the mechanisms of action of these chemicals is needed.

Acknowledgments

The authors thank R. Farmahin and N. Chepelev for reviewing this manuscript. Grant funding was provided by the Health Canada Chemical Management Plan.

References

Ahmed S, Atlas E. 2016. Bisphenol S- and bisphenol A-induced adipogenesis of murine preadipocytes occurs through direct peroxisome proliferator-activated receptor gamma activation. Int J Obes (Lond) 40(10):1566–1573, PMID: 27273607, https://doi.org/10.1038/ijo.2016.95.

Belcher SM, Cookman CJ, Patisaul HB, Stapleton HM. 2014. *In vitro* assessment of human nuclear hormone receptor activity and cytotoxicity of the flame

retardant mixture FM 550 and its triarylphosphate and brominated components. Toxicol Lett 228(2):93–102, PMID: 24786373, https://doi.org/10.1016/j.toxlet.2014.04.017.

Boucher JG, Ahmed S, Atlas E. 2016. Bisphenol S induces adipogenesis in primary human preadipocytes from female donors. Endocrinology 157(4):1397–1407, PMID: 27003841, https://doi.org/10.1210/en.2015-1872.

Boucher JG, Boudreau A, Atlas E. 2014a. Bisphenol A induces differentiation of human preadipocytes in the absence of glucocorticoid and is inhibited by an estrogen-receptor antagonist. Nutr Diabetes 4:e102, PMID: 24418828, https://doi.org/10.1038/nutd.2013.43.

Boucher JG, Husain M, Rowan-Carroll A, Williams A, Yauk CL, Atlas E. 2014b. Identification of mechanisms of action of bisphenol A-induced human preadipocyte differentiation by transcriptional profiling. Obesity (Silver Spring) 22(11):2333–2343, PMID: 25047013, https://doi.org/10.1002/oby.20848.

Dobin A, Davis CA, Schlesinger F, Drenkow J, Zaleski C, Jha S, et al. 2013. STAR: ultrafast universal RNA-seq aligner. Bioinformatics 29(1):15–21, PMID: 23104886, https://doi.org/10.1093/bioinformatics/bts635.

Dodson RE, Perovich LJ, Covaci A, Van den Eede N, Ionas AC, Dirtu AC, et al. 2012. After the PBDE phase-out: a broad suite of flame retardants in repeat house dust samples from California. Environ Sci Technol 46(24):13056–13066, PMID: 23185960, https://doi.org/10.1021/es303879n.

Ducharme NA, Bickel PE. 2008. Lipid droplets in lipogenesis and lipolysis. Endocrinology 149(3):942–949, PMID: 18202123, https://doi.org/10.1210/en.2007-1713.

Fagerholm S, Ortegren U, Karlsson M, Ruishalme I, Strålfors P. 2009. Rapid insulin-dependent endocytosis of the insulin receptor by caveolae in primary adipocytes. PLoS One 4(6):e5985, PMID: 19543529, https://doi.org/10.1371/journal.pone.0005985.

Frisdal E, Le Lay S, Hooton H, Poupel L, Olivier M, Alili R, et al. 2015. Adipocyte ATP-binding cassette G1 promotes triglyceride storage, fat mass growth, and human obesity. Diabetes 64(3):840–855, PMID: 25249572, https://doi.org/10.2337/db14-0245.

Gimble JM, Dorheim MA, Cheng Q, Medina K, Wang CS, Jones R, et al. 1990. Adipogenesis in a murine bone marrow stromal cell line capable of supporting B lineage lymphocyte growth and proliferation: biochemical and molecular characterization. Eur J Immunol 20(2):379–387, PMID: 2178944, https://doi.org/10.1002/eji.1830200222.

Greenspan P, Mayer EP, Fowler SD. 1985. Nile red: a selective fluorescent stain for intracellular lipid droplets. J Cell Biol 100(3):965–973, PMID: 3972906.

Hardie DG, Hawley SA, Scott JW. 2006. AMP-activated protein kinase – development of the energy sensor concept. J Physiol 574(pt 1):7–15, PMID: 16644800, https://doi.org/10.1113/jphysiol.2006.108944.

Hoffman K, Fang M, Horman B, Patisaul HB, Garantziotis S, Birnbaum LS, et al. 2014. Urinary tetrabromobenzoic acid (TBBA) as a biomarker of exposure to the flame retardant mixture Firemaster® 550. Environ Health Perspect 122(9):963–969, PMID: 24823833, https://doi.org/10.1289/ehp.1308028.

Inoue J, Kumagai H, Terada T, Maeda M, Shimizu M, Sato R. 2001. Proteolytic activation of SREBPs during adipocyte differentiation. Biochem Biophys Res Commun 283(5):1157–1161, PMID: 11355894, https://doi.org/10.1006/bbrc.2001.4915.

Janderová L, McNeil M, Murrell AN, Mynatt RL, Smith SR. 2003. Human mesenchymal stem cells as an *in vitro* model for human adipogenesis. Obes Res 11(1):65–74, PMID: 12529487, https://doi.org/10.1038/oby.2003.11.

Kawaguchi N, Sundberg C, Kveiborg M, Moghadaszadeh B, Asmar M, Dietrich N, et al. 2003. ADAM12 induces actin cytoskeleton and extracellular matrix reorganization during early adipocyte differentiation by regulating β1 integrin function. J Cell Sci 116(pt 19):3893–3904, PMID: 12915587, https://doi.org/10.1242/jcs.00699.

Klemm DJ, Roesler WJ, Boras T, Colton LA, Felder K, Reusch JE. 1998. Insulin stimulates cAMP-response element binding protein activity in HepG2 and 3T3-L1 cell lines. J Biol Chem 273(2):917–923, https://doi.org/10.1074/jbc.273.2.917.

Krey G, Braissant O, L'Horset F, Kalkhoven E, Perroud M, Parker MG, et al. 1997. Fatty acids, eicosanoids, and hypolipidemic agents identified as ligands of peroxisome proliferator-activated receptors by coactivator-dependent receptor ligand assay. Mol Endocrinol 11(6):779–791, PMID: 9171241, https://doi.org/10.1210/mend.11.6.0007.

Lam JC, Lau RK, Murphy MB, Lam PK. 2009. Temporal trends of hexabromocyclododecanes (HBCDs) and polybrominated diphenyl ethers (PBDEs) and detection of two novel flame retardants in marine mammals from Hong Kong, South China. Environ Sci Technol 43(18):6944–6949, PMID: 19806725.

Lane MD, Lin FT, MacDougald OA, Vasseur-Cognet M. 1996. Control of adipocyte differentiation by CCAAT/enhancer binding protein alpha (C/EBP alpha). Int J Obes Relat Metab Disord 20 (suppl 3):S91–S96, PMID: 8680485.

Langmead B, Salzberg SL. 2012. Fast gapped-read alignment with Bowtie 2. Nat Methods 9(4):357–359, PMID: 22388286, https://doi.org/10.1038/nmeth.1923.

Leto D, Saltiel AR. 2012. Regulation of glucose transport by insulin: traffic control of GLUT4. Nat Rev Mol Cell Biol 13(6):383–396, PMID: 22617471, https://doi.org/10.1038/nrm3351.

Liu YY, Ayers S, Milanesi A, Teng X, Rabi S, Akiba Y, et al. 2015. Thyroid hormone receptor sumoylation is required for preadipocyte differentiation and proliferation. J Biol Chem 290(12):7402–7415, PMID: 25572392, https://doi.org/10.1074/jbc.M114.600312.

Mori T, Sakaue H, Iguchi H, Gomi H, Okada Y, Takashima Y, et al. 2005. Role of Krüppel-like factor 15 (KLF15) in transcriptional regulation of adipogenesis. J Biol Chem 280(13):12867–12875, PMID: 15664998, https://doi.org/10.1074/jbc.M410515200.

Nagai H, Ebisu S, Abe R, Goto T, Takahashi N, Hosaka T, et al. 2011. Development of a novel PPARγ ligand screening system using pinpoint fluorescence-probed protein. Biosci Biotechnol Biochem 75(2):337–341, PMID: 21307572, https://doi.org/10.1271/bbb.100810.

Parsons SA, Sharma R, Roccamatisi DL, Zhang H, Petri B, Kubes P, et al. 2012. Endothelial paxillin and focal adhesion kinase (FAK) play a critical role in neutrophil transmigration. Eur J Immunol 42(2):436–446, PMID: 22095445, https://doi.org/10.1002/eji.201041303.

Patisaul HB, Roberts SC, Mabrey N, McCaffrey KA, Gear RB, Braun J, et al. 2013. Accumulation and endocrine disrupting effects of the flame retardant mixture Firemaster® 550 in rats: an exploratory assessment. J Biochem Mol Toxicol 27(2):124–136, PMID: 23139171, https://doi.org/10.1002/jbt.21439.

Phillips AL, Chen A, Rock KD, Horman B, Patisaul HB, Stapleton HM. 2016. Editor's highlight: transplacental and lactational transfer of Firemaster® 550 components in dosed Wistar rats. Toxicol Sci 153(2):246–257, PMID: 27370412, https://doi.org/10.1093/toxsci/kfw122.

Pillai HK, Fang M, Beglov D, Kozakov D, Vajda S, Stapleton HM, et al. 2014. Ligand binding and activation of PPARγ by Firemaster® 550: effects on adipogenesis and osteogenesis *in vitro*. Environ Health Perspect 122(11):1225–1232, PMID: 25062436, https://doi.org/10.1289/ehp.1408111.

Reusch JE, Colton LA, Klemm DJ. 2000. CREB activation induces adipogenesis in 3T3-L1 cells. Mol Cell Biol 20(3):1008–1020, PMID: 10629058.

Robinson MD, McCarthy DJ, Smyth GK. 2010. edgeR: a bioconductor package for differential expression analysis of digital gene expression data. Bioinformatics 26(1):139–140, PMID: 19910308, https://doi.org/10.1093/bioinformatics/btp616.

Robinson MD, Oshlack A. 2010. A scaling normalization method for differential expression analysis of RNA-seq data. Genome Biol 11(3):R25, PMID: 20196867, https://doi.org/10.1186/gb-2010-11-3-r25.

Stapleton HM, Allen JG, Kelly SM, Konstantinov A, Klosterhaus S, Watkins D, et al. 2008. Alternate and new brominated flame retardants detected in U.S. house dust. Environ Sci Technol 42(18):6910–6916, PMID: 18853808.

Tomlinson JJ, Boudreau A, Wu D, Abdou Salem H, Carrigan A, Gagnon A, et al. 2010. Insulin sensitization of human preadipocytes through glucocorticoid hormone induction of forkhead transcription factors. Mol Endocrinol 24(1):104–113, PMID: 19887648, https://doi.org/10.1210/me.2009-0091.

Tomlinson JJ, Boudreau A, Wu D, Atlas E, Haché RJ. 2006. Modulation of early human preadipocyte differentiation by glucocorticoids. Endocrinology 147(11):5284–5293, PMID: 16873539, https://doi.org/10.1210/en.2006-0267.

Tung EWY, Ahmed S, Peshdary V, Atlas E. 2017. Firemaster® 550 and its components isopropylated triphenyl phosphate and triphenyl phosphate enhance adipogenesis and transcriptional activity of peroxisome proliferator activated receptor (Pparγ) on the adipocyte protein 2 (aP2) promoter. PLoS One 12(4):e0175855, PMID: 28437481, https://doi.org/10.1371/journal.pone.0175855.

van der Deure WM, Peeters RP, Visser TJ. 2010. Molecular aspects of thyroid hormone transporters, including MCT8, MCT10, and OATPs, and the effects of genetic variation in these transporters. J Mol Endocrinol 44(1):1–11, PMID: 19541799, https://doi.org/10.1677/JME-09-0042.

Verstraeten VL, Renes J, Ramaekers FC, Kamps M, Kuijpers HJ, Verheyen F, et al. 2011. Reorganization of the nuclear lamina and cytoskeleton in adipogenesis. Histochem Cell Biol 135(3):251–261, PMID: 21350821, https://doi.org/10.1007/s00418-011-0792-4.

Yeh WC, Bierer BE, McKnight SL. 1995. Rapamycin inhibits clonal expansion and adipogenic differentiation of 3T3-L1 cells. Proc Natl Acad Sci U S A 92(24):11086–11090, PMID: 7479942.